05

Investigation of the processes of formation of the crystalline phase in rapid-quenched layered amorphous-crystalline ribbons produced of $Ti_{50}Ni_{25}Cu_{25}$ alloy during electric pulse treatment

© N.N. Sitnikov[1,2], S.V. Greshnyakova[1], I.A. Zaletova[1], A.V. Shelyakov[2]

[1] State Scientific Center of the Russian Federation „Keldysh Research Center", Moscow, Russia
[2] National Research Nuclear University „MEPhI," Moscow, Russia
E-mail: sitnikov_nikolay@mail.ru

Received November 27, 2024
Revised January 19, 2025
Accepted January 29, 2025

The effect of electric pulse treatment (EPT) on the microstructure of rapid-quenched layered amorphous-crystalline ribbons obtained by spinning a $Ti_{50}Ni_{25}Cu_{25}$ melt on a rapid rotating copper disk has been experimentally investigated. A sequential series of samples of $Ti_{50}Ni_{25}Cu_{25}$ alloy ribbons was obtained after EPT with a single pulse of electric current with a duration of 1 ms with an increase in the degree of heating after reaching the recrystallization temperature of the amorphous part of the ribbons at an electric current density (J) from 680 to 891 A/mm^2. Studies of the microstructure of the cross-section of the treated samples and the calorimetric effects during the course of martensitic transformations (MT) have shown that the magnitude and nature of MT are consistent with the observed microstructure of ribbons after EPT with varying degrees of annealing. An increase in J during EPT and overheating leads to the formation of a more homogeneous crystal structure, characterized mainly by columnar crystals, and an increase in MT temperature. The peak temperature of the austenitic transformation in the treated samples, depending on the increase in J, increases from 39.0 °C in the initial state to 64.5 °C at $J = 891$ A/mm^2.

Keywords: electric pulse treatment, amorphous state, crystalline state, TiNiCu, phase transition.

DOI: 10.61011/0000000000

Ultrarapid quenching (melt spinning) methods allow one to obtain unique structural states of various materials by achieving high cooling rates [1–3]. A ribbon with a layered amorphous-crystalline structure may be produced when the quasi-binary TiNi–TiCu system melt is cooled at rates ranging from 10^5 to 10^6 °C/s. The layered amorphous-crystalline composite synthesized this way in the form of a thin ribbon has a peculiar physical and mechanical property: the two-way shape memory effect (TWSME) with bending deformation during thermal cycling within the range of reversible martensitic transformation (MT) [4]. Unique layered structural composites with TWSME have potential for application in micromechanics, with one of the striking examples being microgrippers of various purpose [4–6].

Rapid-quenched layered amorphous-crystalline ribbons may be subjected to further processing of various kinds to obtain new properties and modify existing shape memory effects. The most common options for processing the amorphous state are thermal, thermomechanical, cryogenic, laser treatment, etc. [7,8]. Electric pulse treatment (EPT), which involves passing a single pulse (or a series of short pulses) of electric current through a sample (ribbon), is one of the promising techniques of heat treatment without temperature holding. Electric current provides an opportunity to heat thin samples in a short time and perform crystallization virtually without isothermal holding. This dynamic crystallization leads to the formation of new structural states of rapid-quenched alloys [9,10].

The aim of the present study is to examine the processes of formation of the crystalline phase during EPT of rapid-quenched layered amorphous-crystalline ribbons of the $Ti_{50}Ni_{25}Cu_{25}$ alloy and their influence on martensitic transformations.

The chosen $Ti_{50}Ni_{25}Cu_{25}$ (at.%) alloy has a pronounced tendency to amorphization and a shape memory effect in the crystalline state. The prepared ligature was melted in a quartz crucible and injected onto the surface of a rapidly rotating copper disk by planar casting. The cooling rate of the melt was close to $4 \cdot 10^5$ °C/s. Thin layered amorphous-crystalline ribbons with an approximate thickness of 40 μm were obtained as a result.

EPT was carried out using a laboratory setup by passing a single electric current pulse with a given amplitude and duration through the processed ribbon sample. The processing method and the mentioned setup allow for dosed heating of ribbon samples over a time of 0.1–100 ms. The calculation formula relating the required thermal energy of an electric pulse (via current density J) to the duration of electric current treatment and the sample parameters was presented in [10]. The temperature to which the ribbon must be heated was taken to be equal to the crystallization peak temperature of the amorphous ribbon part (454 °C), which was determined by differential scanning calorimetry

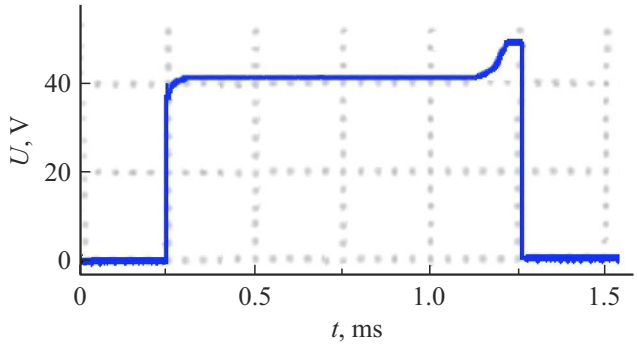

Figure 1. Oscilloscope record of voltage characterizing the degree of heating of the sample during EPT and the transition from an amorphous state to a crystalline one.

(DSC) at a heating rate of 10 °C/min. It was calculated that J of about 819 A/mm^2 is needed to heat ribbon samples with an approximate length of 20 mm to a temperature of 454 °C in 1 ms. The obtained J value is an estimate, and the degree of underheating or overheating of the samples in the EPT process was varied relative to it.

To assess the degree of underheating and overheating of samples during EPT, the change in potential difference at the processed sample, which reflects the variation of its electric resistance in transition of the amorphous ribbon part to a crystalline state, was recorded with an oscilloscope. When a temperature close to the devitrification one is reached and the amorphous phase transitions to a crystalline state, the resistance of the processed sample decreases. The state of „optimum“ (in terms of energy input) crystallization is characterized by the dynamics of variation of the electric resistance shown in Fig. 1. The signal increases in the right part of the pulse in the oscilloscope record, eventually reaching a constant level („plateau“). If the energy input is greater than that required to heat the sample to the crystallization temperature of the amorphous ribbon part, the signal increases in the middle or left parts of a pulse. When the energy input is insufficient to heat the sample to the crystallization temperature, the Π-shaped pulse form remains unchanged; in the case of heating to partial crystallization, the signal rises without the transition to a constant level in the oscilloscope record.

A series of processed (annealed) samples crystallized completely or partially at J varying from 680 to 891 A/mm^2 were obtained as a result of EPT of amorphous-crystalline ribbons.

Studies of the microstructures of cross sections of the obtained experimental samples revealed that the as-prepared ribbon is characterized by a layered amorphous-crystalline structure with a crystalline layer with an approximate thickness of 10 μm and an amorphous layer with a thickness close to 30 μm (Fig. 2, *a*). The microstructure of ribbon samples subjected to EPT changes depending on the energy input (see Figs. 2, *b*–*e*). With EPT at J below 758 A/mm^2, no new crystalline phases form in the amorphous layer (Fig. 2, *b*). The crystalline layer does not undergo any noticeable structural changes. With an increase in J, the crystalline phase starts forming in the amorphous layer from its boundaries and in the bulk (Fig. 2, *c*). A structure of columnar crystals is observed at the boundaries of the amorphous layer, and individual or grouped spherical crystals are found in the bulk.

At $J = 784$ A/mm^2 or more, a completely crystalline microstructure with a non-uniform distribution of crystals across its thickness is observed: a structure of columnar crystals forms near the ribbon surfaces, and individual or grouped large crystals are present in the bulk (Figs. 2, *d*, *e*). Columnar crystals from the initial crystalline layer at the non-contact ribbon surface grow in size toward the inner part of the ribbon to crystals formed inside the amorphous phase. As the EPT energy input increases, the fraction of columnar crystals grows (Fig. 2, *e*), and columnar crystals come into contact with each other in certain regions in the middle part of the ribbon. At $J = 891$ A/mm^2, the fraction of columnar crystals in contact with each other becomes dominant (Fig. 2, *f*), and isolated lens-shaped crystals are found between some of them in the middle part of the ribbon. It follows from the obtained data that the EPT mode with crystallization in the intermediate region of a pulse and subsequent overheating leads to the formation of a crystalline structure dominated by columnar crystals.

The examination of samples after EPT by DSC at a heating rate of 5 °C/min demonstrated that an increase in J from 680 to 891 A/mm^2 leads to a consistent increase in temperature of the reverse MT (austenitic transformation) and a change in enthalpy (ΔH) during the MT (Fig. 3). The temperature of the austenitic transformation peak (A_p) in the processed samples increases with J from 39.0 °C in the as-prepared state to 64.5 °C at $J = 891$ A/mm^2. It can be seen from the obtained DSC heating curves that although structural changes are lacking at J below 758 A/mm^2, certain differences in the nature of MT in the crystalline layer and an increase in ΔH (-2.2 J/g) are noticeable. The DSC curve for the sample treated with J below 775 A/mm^2 is characterized by a more pronounced austenite transformation peak and $\Delta H = -7.0$ J/g, which corresponds to the observed structure with partial crystallization of the amorphous phase. The samples processed with J ranging from 784 to 891 A/mm^2 are characterized by a completely crystallized state and, accordingly, the highest ΔH values (close to -10 J/g). The MT peak broadening in partially and completely crystallized samples and the two-stage nature of the MT process in the samples processed with $J = 784$ and 819 A/mm^2, which reflects the bimorphic distribution of crystals in the ribbon structure, were noted (Figs. 2, *d*, *e*). In the sample with $J = 891$ A/mm^2, the heat absorption peak is slightly narrower, which agrees well with the observed microstructure that is more homogeneous and dominated by columnar crystals (Fig. 2, *f*). The increase in MT temperatures with an increase in energy of an EPT pulse may be attributed to the expansion of boundaries of structural elements and the emergence of strain that

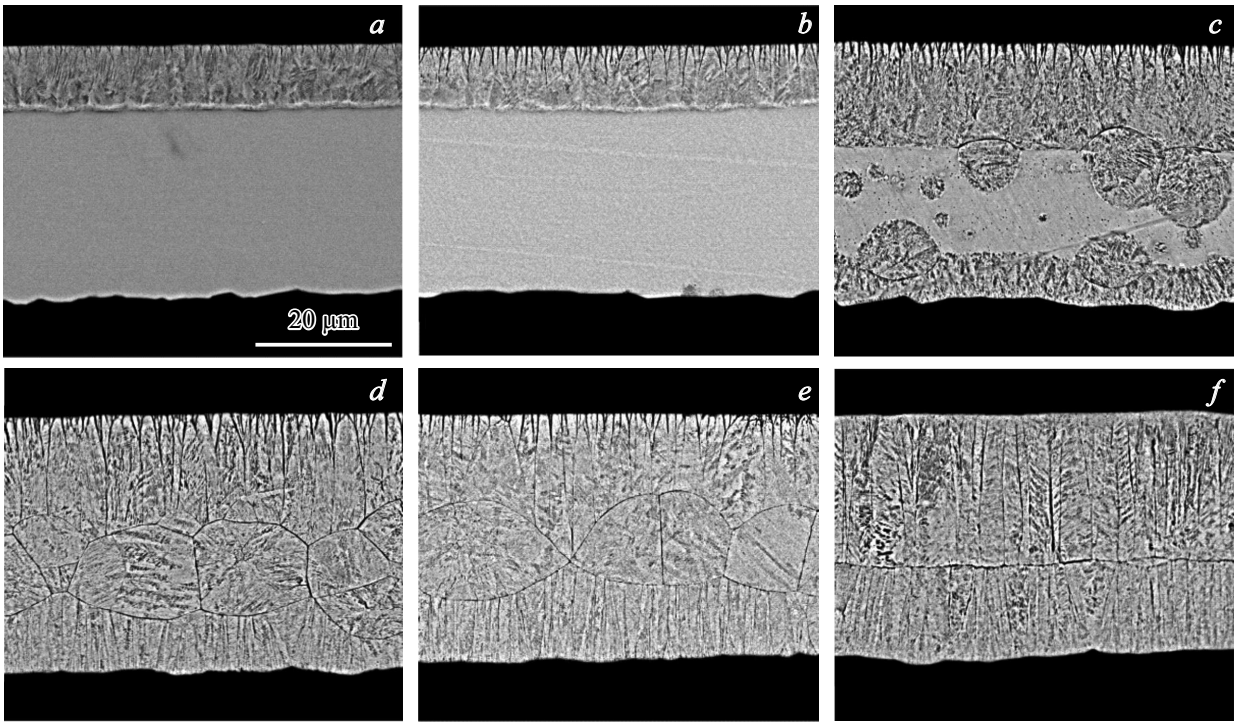

Figure 2. Scanning electron microscopy images of cross sections of amorphous-crystalline ribbons of the $Ti_{50}Ni_{25}Cu_{25}$ alloy in the as-prepared state (prior to processing) (*a*) and after EPT with $J = 713$ (*b*), 775 (*c*), 784 (*d*), 819 (*e*), and 891 A/mm^2 (*f*).

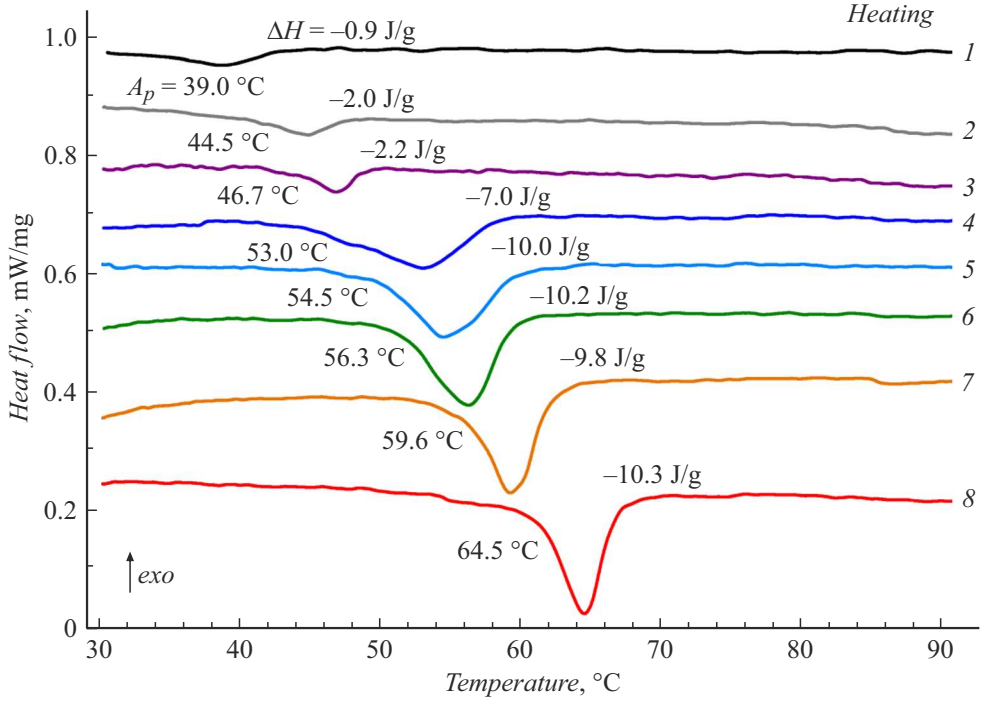

Figure 3. DSC heating curves of ribbon samples of the $Ti_{50}Ni_{25}Cu_{25}$ alloy in the initial amorphous-crystalline state (prior to processing) (*1*) and after EPT with $J = 713$ (*2*), 758 (*3*), 775 (*4*), 784 (*5*), 819 (*6*), 860 (*7*), and 891 A/mm^2 (*8*).

interferes with the MT (not least because of the possible formation of Ti–Cu phases in the case of overheating).

The obtained data demonstrate clearly the agreement between the magnitude and nature of calorimetric effects during the MT and the observed microstructure of ribbons after EPT with varying degrees of annealing.

An increase in energy of an EPT pulse and the degree of overheating after crystallization of the amorphous state

leads to the formation of a more homogeneous crystalline structure, which is dominated by columnar crystals, and an increase in temperature of the MT.

Funding

This study was supported by a grant from the Russian Science Foundation (project No. 24-22-00035).

Conflict of interest

The authors declare that they have no conflict of interest.

References

[1] A.M. Glezer, Phys. Usp., **55** (5), 522 (2012). DOI: 10.3367/UFNe.0182.201205h.0559.
[2] R.V. Sundeev, A.V. Shalimova, N.N. Sitnikov, O.P. Chernogorova, A.M. Glezer, M.Yu. Presnyakov, I.A. Karateev, E.A. Pechina, A.V. Shelyakov, J. Alloys Compd., **845**, 156273 (2020). DOI: 10.1016/j.jallcom.2020.156273
[3] S. Wang, X. Chi, J.-B. Sun, H.-W. Ding, W. Yang, Mater. Lett., **361**, 136124 (2024). DOI: 10.1016/j.matlet.2024.136124
[4] A. Shelyakov, N. Sitnikov, K. Borodako, V. Koledov, I. Khabibullina, S. von Gratowski, J. Micro-Bio Robot., **16** (1), 43 (2020). DOI: 10.1007/s12213-020-00126-3
[5] I. Stachiv, E. Alarcon, M. Lamac, Metals, **11** (3), 415 (2021). DOI: 10.3390/met11030415
[6] S.V. von Gratowski, M.I. Zhukovskaya, A.M. Lunichkin, A.V. Shelyakov, N.N. Sitnikov, V.V. Koledov, K.A. Borodako, S.F. Petrenko, Tech. Phys., **68** (8), 1135 (2023). DOI: 10.61011/TP.2023.08.57277.37-23.
[7] A. El Boubekri, M. Ounacer, M. Sajieddine, M. Sahlaoui, H. Lassri, A. Essoumhi, E.K. Hlil, A. Razouk, E. Agouriane, Physica B, **663**, 414997 (2023). DOI: 10.1016/j.physb.2023.414997
[8] J. Jiang, Y. Wu, H. Chen, Z. Wan, D. Ding, L. Xia, X. Guo, P. Yu, J. Colloid Interface Sci., **633**, 303 (2023). DOI: 10.1016/j.jcis.2022.11.081
[9] A. Shelyakov, N. Sitnikov, I. Khabibullina, N. Tabachkova, V. Fominski, N. Andreev, Mater. Lett., **248**, 48 (2019). DOI: 10.1016/j.matlet.2019.03.140
[10] N.N. Sitnikov, I.A. Zaletova, A.V. Shelyakov, A.A. Ashmarin, Met. Sci. Heat Treat., **63** (5-6), 251 (2021). DOI: 10.1007/s11041-021-00679-5

Translated by D.Safin